Article citation info:
GÓMEZ CQM, GARCÍA FPM, JIMENEZ AJ, CHENG L, KOGIA M, MOHIMI A, PAPAELIAS M. A heuristic method for detecting and locating faults employing electromagnetic acoustic transducers. Eksploatacja i Niezawodnosc – Maintenance and Reliability 2017; 19 (4): 493–500, http://dx.doi.org/10.17531/ein.2017.4.1.

Carlos Quiterio GÓMEZ Muñoz
Fausto Pedro GARCÍA Marquez
Alfredo ARCOS Jimenez
Liang CHENG
Maria KOGIA
Abbas MOHIMI
Mayorkinos PAPAELIAS

A HEURISTIC METHOD FOR DETECTING AND LOCATING FAULTS EMPLOYING ELECTROMAGNETIC ACOUSTIC TRANSDUCERS

HEURYSTYCZNA METODA WYKRYWANIA I LOKALIZOWANIA USTEREK Z WYKORZYSTANIEM ELEKTROMAGNETYCZNYCH PRZETWORNIKÓW AKUSTYCZNYCH

The objective of this paper is to demonstrate a novel signal processing for detection, identification and flaw sizing of structural damage using ultrasonic testing with Electromagnetic Acoustic Transducers (EMATs). Damage detection involves the recognition of a defect that exists within a structure. Damage location is the identification of the geometric position of the defect. Defect classification is the cluster of the damage type into multiple damage scenarios. In the absence of external interferences, a good measure of detectability of a flaw is its signal-to-noise ratio (SNR). Although the SNR depends on various parameters such as electronics used, material properties, e.g. homogeneity and damping, and flaw size, it can be improved using advanced signal processing. The main scientific novelties presented in this paper focus on filtering signal noise through advanced digital signal processing; incorporating wavelet transforms for image and signal representation enhancements; investigating multi-parametric analysis for noise identification and defect classification; studying attenuation curves properties for defect localisation improvement and flaw sizing and location algorithm development.

Keywords: *fault detection and diagnosis, electromagnetic acoustic transducers (EMAT), wavelet transforms, non destructive tests, guided waves.*

Celem niniejszego artykułu jest omówienie nowatorskiego sposobu przetwarzania sygnałów w celu wykrywania, identyfikacji i oceny uszkodzeń strukturalnych przy użyciu ultrasonograficznych testów za pomocą elektromagnetycznych przetworników akustycznych (EMAT). Wykrywanie uszkodzeń polega na rozpoznaniu istniejących defektów wewnątrz danej struktury. Lokalizacja uszkodzeń sprowadza się do identyfikacji geometrycznego położenia defektu. Klasyfikacja defektu to klaster typu uszkodzenia w wielu scenariuszach uszkodzeń. W przypadku braku zewnętrznych zakłóceń, dobrym wskaźnikiem wykrywalności błędu jest stosunek sygnału do szumu (SNR). Pomimo tego, że SNR zależy od różnych parametrów, takich jak użyta elektronika, właściwości materiału, np. jednorodność i tłumienie, a także wielkość wady, wskaźnik ten można poprawić przy użyciu zaawansowanego przetwarzania sygnałów. Główne nowe zagadnienia naukowe przedstawione w niniejszym artykule skupiają się na filtrowaniu szumu sygnału za pomocą zaawansowanego przetwarzania sygnału cyfrowego, w tym wykorzystując transformaty falkowe w celu ulepszenia obrazu i sygnału; badanie analizy wieloparametrycznej w celu identyfikacji szumów i klasyfikacji defektów; badanie właściwości krzywych osłabiania w celu sprawniejszego wykrywania i oceny wad oraz rozwoju algorytmu lokalizacji.

Słowa kluczowe: *wykrywanie i diagnozowanie wad, elektromagnetyczne przetworniki akustyczne, EMAT, transformaty falkowe, badania nieniszczące, fale prowadzone.*

1. Introduction

Non-destructive testing (NDT) for fault detection in structures has received more attention in recent years. Significant advances in instrumentation technology and digital signal processing have been made [16, 17, 19, 25, 30]. Signal processing methods together with structural health monitoring (SHM) permit the identification and diagnosis of faults and their location based on changes in static and

dynamic structural features [14, 22, 23]. In addition, these techniques can be remotely controlled and they should work online, resulting in a reduction of costs associated to manual inspections, downtimes, etc. [11, 20, 28].

Guided waves are a common technique employed for SHM within the NDT field, being particularly useful for structural components based on plate or tube geometries. The technique is based on the excitation of low frequency ultrasonic waves propagating along a structure such as a pipeline over long distances, allowing inspection of large areas without any relocation of the transducers.

The purpose of this paper is to demonstrate a novel fault detection and diagnosis (FDD) approach using ultrasound inputs in conjunction with advanced signal processing methods [4, 10, 21, 31] for monitoring the structural condition of a steel plate. The novel signal processing is based on system identification techniques in discrete time to estimate potential faults. The wavelet and Hilbert transforms are employed to work in conjunction with an automatic peak detection algorithm [5]. The algorithm detects which peaks correspond to echoes from the edges, and which correspond to potential defects. Once a potential crack is detected, the algorithm shows the exact location of the defect, and the crack size is compared with the attenuation curve.

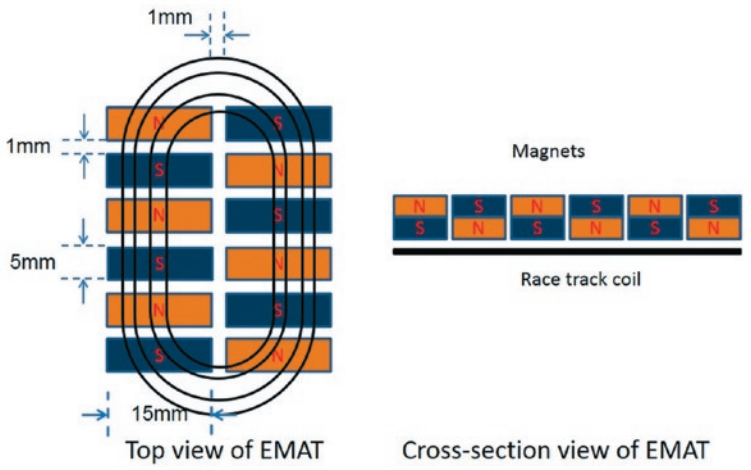

Fig. 2. Configuration of EMAT transducer

2. Electromagnetic acoustic transducers for condition monitoring

The electromagnetic acoustic transducer (EMAT) is a transducer for non-contact sound generation and reception using magnetostrictive phenomena and the interaction of the Lorenz force with the crystal lattice of the material being inspected. EMATs have been widely used in non-destructive testing in the generation of Shear and Lamb waves [3, 33]. In this study EMATs manufactured by SONEMAT Limited in the UK (Figure 1) have been used to carry out the experiments of interests. The EMATs employed use a specific coil and magnet configuration appropriate for the tests carried out [27].

A 3 mm thickness plate of 316Ti stainless steel has been employed for the experiments. The EMATs incorporate a race track coil with periodic permanent magnet to generate shear waves (SH0 mode) in the plate. The dimension of each EMAT is 15 mm x 5 mm x 5 mm. The distance between the magnets is 1 mm and the magnetic strength of each magnet is 0.3 T. The diameter of the coil is 0.315 mm, the width 15 mm and length 35 mm, with a lift-off distance of 0.1 mm from the samples surface. The EMAT configuration is shown in the schematic of Figure 2.

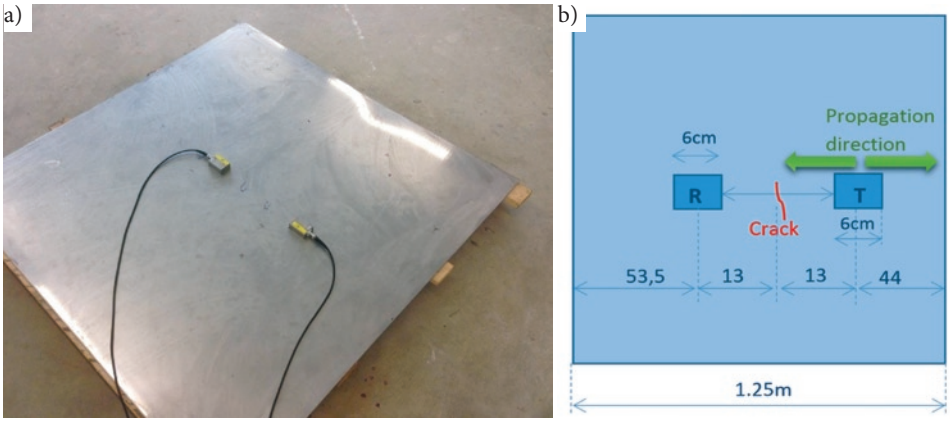

Fig. 3. Actuator and sensor placement in the plate (a) and scheme of the defect location (b).

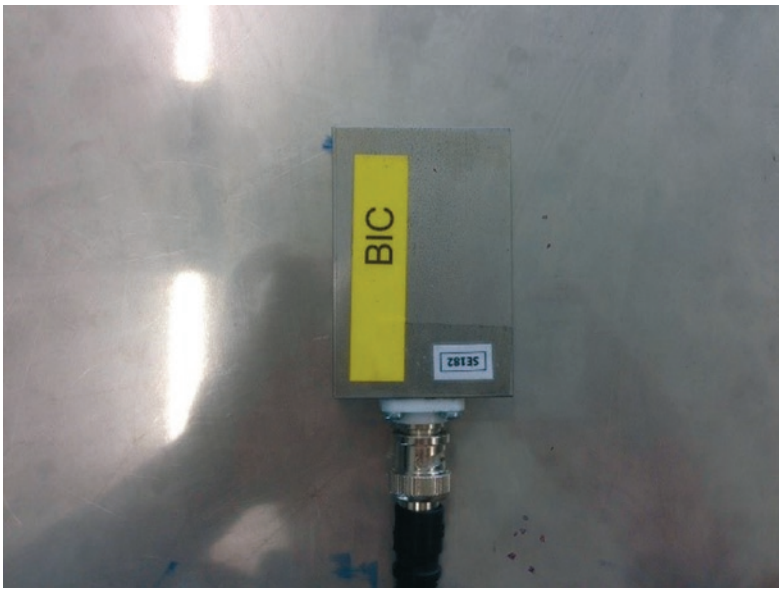

Fig. 1. Electromagnetic Acoustic Transducer manufactured by SONEMAT Limited in the UK

This type of EMAT configuration is applicable for the detection of transverse defects, such as spiral cracking, blow-out holes, circumferential cracking, bell splitting, etc. Since 316Ti stainless steel has an austenitic microstructure it is paramagnetic and therefore, magnetostriction is not relevant. Ultrasonic waves are produced due to the Lorentz forces acting normal to the plate surface producing ultrasonic waves propagating along the longitudinal direction of the test plate.

3. Experimental Tests

An artificial defect has been induced in the plate using spark erosion to carry out automatic detection and location of defects. Figure 3 shows the experimental configuration employed. The EMAT is excited by a 256 kHz and six-cycle pulse. Shear waves are generated in both directions. The

EMAT (R) receives echoes from the edges and from the crack. Figure 4 shows the four first reflections produced by the boundaries.

Shear waves are non-dispersive signals, i.e. the propagation velocity of these waves is not frequency dependent. The propagation velocity of shear waves depends on the material properties [32]. For the 3 mm austenitic steel plate (316Ti) considered herewith the shear wave velocity is 3020 m/s.

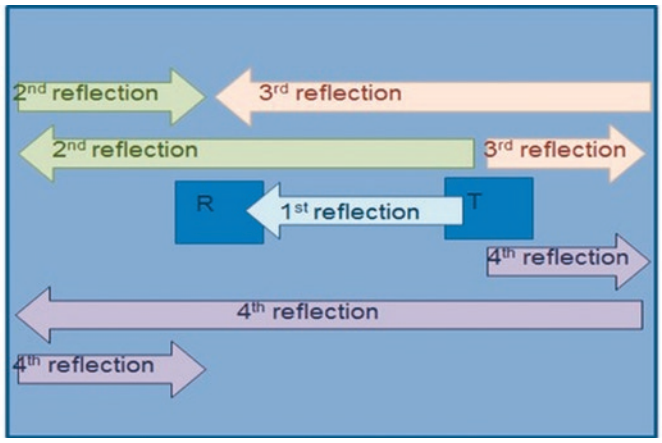

Fig. 4. Reflections from the edges registered by sensor (R)

4. Signal processing

This section presents a novel method based on a wavelet-based algorithm that has been applied to the signals from the EMATs to improve the SNR. A pre-filter has been implemented to extract the low frequency information of the EMAT signals, where it reduces the unexpected frequency components of signals. Then a denoising algorithm has been applied to improve the SNR without introducing time delay in the original signals [15].

4.1. Wavelet pre-filter and de-noising.

The wavelet transform is an analysis method which can be employed to identify the local characteristics of a signal in the time and frequency domain, e.g. with the use of a series of decomposition coefficients at different frequency bands [6, 10]. It is recommended for large time intervals where great accuracy is required at low frequencies and vice versa, e.g. small regions where precision details are required at higher frequencies [7]. The wavelet transform is also a useful method to characterise and identify signals with spectral features, unusual temporary files and other properties related to non-standing waves.

Wavelet transforms are an alternative to the fast Fourier transform (FFT), or to the short-time Fourier transform,

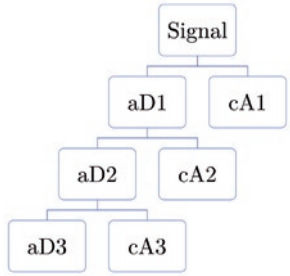

Fig. 5. Wavelet decompositions tree

to obtain results in the time domain [13] and [24]. The signal processing from the time domain to the frequency domain usually implies loss of information, being difficult to determine the appearance of specific frequencies [26].

Signals are divided therefore into low frequency *approximations* (**A**) and high frequency *details* (**D**), where the sum of **A** and **D** is always equal to the original signal. The division is done using low pass and high pass filters [2]. In order to reduce the computational and mathematical costs due to the data duplication, a sub-sampling is usually implemented, containing the half of the collected information from **A** and **D** without losing information.

In the case of the multi-level filters, they repeat the filtering process with the output signals from the previous level. This leads to the wavelet decomposition trees (Figure 5) [1, 9]. Additional information is obtained by filtering at each level. However more decompositions levels do not always mean more accurate results.

The objective of the signal pre-processing is to extract the most important information of the original signal before carrying out signal de-noising. It generates new signals adjusted for the application of filters, providing more robust results and greater similarity between signals obtained under different conditions.

The first filter used to prepare the signal has been employing a Daubechies wavelet transform. Daubechies wavelets were used because they handle with boundary problems for finite length signals, being their biggest advantage over other families [12, 29] and [34].

The decomposition five D5 contains more information of the original signal and a lower signal noise ratio without delay regarding to the original signal.

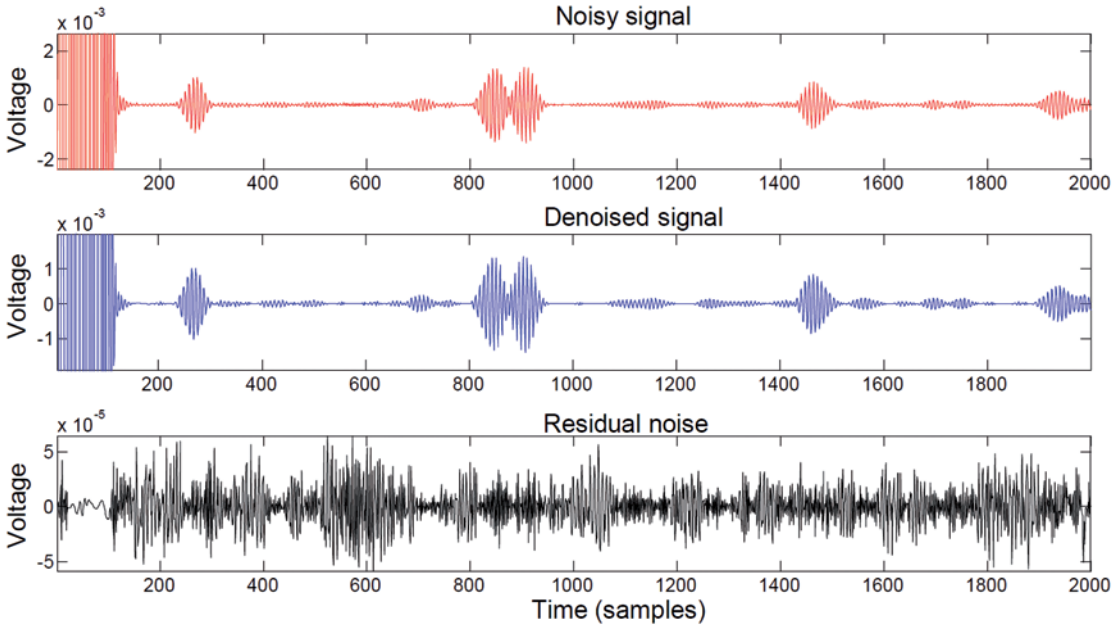

Fig. 6. Decomposition detail five (D5), De-noised D5 and extracted residual noise

Effective filtering should not eliminate any information about the defects, e.g. the peaks with low amplitudes, because it is likely that any of these peaks can be due to a defect. This section describes the approach considered in order to remove noise without compromising the detection of a smaller defect.

The denoising of the signal is performed employing a multilevel 1-D wavelet analysys using Daubechies family. The wavelet decomposition structure of the signal to be de-noised is extracted. The threshold for the de-noising is obtained by a wavelet coefficients selection rule using a penalization method provided by Birgé-Massart. An overly aggressive filtering could eliminate data of interest, such as small echoes that come from defects. Figure 6 shows the original signal and the de-noised signal when it is applied the wavelet de-noised filter. In contrast to other digital filters, the Wavelet de-noising filter does not produce an unwanted signal delay.

It is observed that the filter removes noise significantly, and also does not eliminate information that is related to different structural features.

4.2. Finding events within the signal: Envelope and smooth

Hilbert Transform is employed to obtain the envelope of the filtered signal. It is necessary to smooth the envelope with the aim of finding events in the signal, which usually appear as peaks, i.e. it is desired do not find false alarms. An inadequate window size could produce distortions as "sawtooth" in the signal.

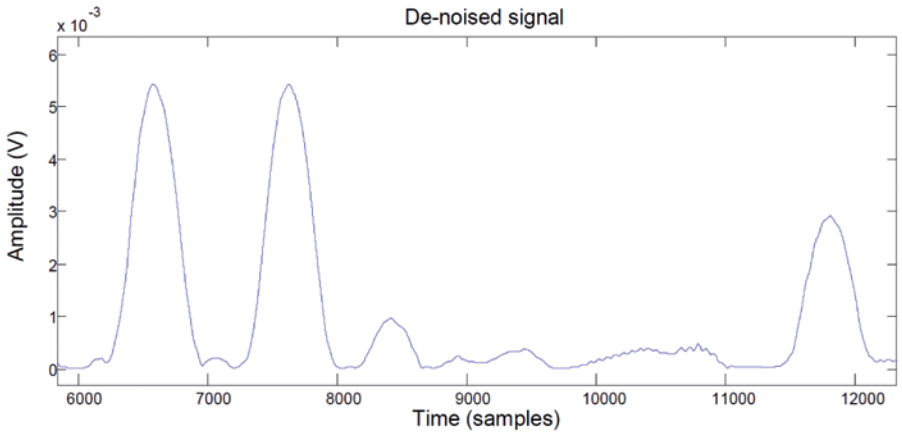

Fig. 7. Smooth of the envelope using Wavelet low pass filter

A good result is achieved by applying again a Wavelet de-noising filter and selecting the low frequency decompositions (approximations). This produces a smoothed function without significantly altering the signal (Figure 7).

4.3. Cracks detection and edges location

The approach identifies the events from the signals that are obtained from elements as boundaries or welds. This process consists of the following steps (see Figure 8):

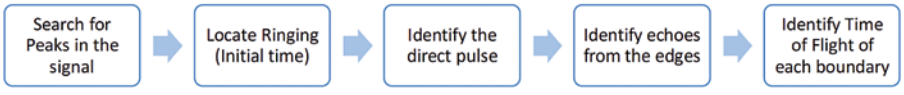

Fig. 8. Identification of edges echoes algorithm

- *Peak search*: It is important to select a proper threshold for this purpose.
- *Identify echoes from the edges*: The time of flight of each echo is obtained and compared with the distances of the sensor and actuator regard to the boundaries.
- *Theoretical and experimental comparison for identification of the boundaries* (Figure 9).

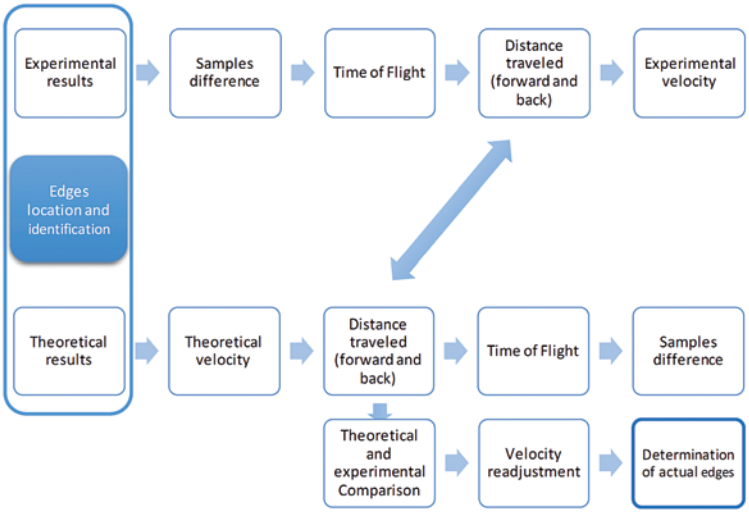

Fig. 9. Theoretical and experimental comparison for edges identification

The obtained information allows the discarding of false cracks, and also provides information such as the attenuation of the ultrasonic wave propagation along the material. The algorithm uses the distance of the EMATs from the edges to perform a self-identification of signal events. The event is located theoretically when the two possible ways of propagation of ultrasound, forward and reverse, are analysed together, taking into account the time of flight (ToF) of each echo. Then the algorithm correlates the theoretical events with the potential events detected in the signal. Finally, the measurement accuracy is checked and validated or not, and each specific event is experimentally located, and obtaining the experimental propagation velocity.

Vector $\mathbf{X}$ contains the position values of the peaks obtained experimentally, $\mathbf{Y}$ the height of the peaks of $\mathbf{X}$, and $\mathbf{X}^*$ the position values of the peaks obtained theoretically.

$$\mathbf{X} = [x_1, \cdots, x_i, \ldots x_n]$$

$$\mathbf{Y} = [y_1, \cdots, y_i, \ldots y_n]$$

$$\mathbf{X}^* = [x_1^*, \cdots, x_j^*, \ldots x_m^*]$$

The matrix $\mathbf{C}$, given by equation (1) contains the absolute difference between each value of $\mathbf{X}$ and each value of $\mathbf{X}^*$

$$\mathbf{C}=\begin{bmatrix} \left|x_1-x_1^*\right| & \cdots & \left|x_1-x_j^*\right| & \cdots & \left|x_1-x_m^*\right| \\ \vdots & & \vdots & & \vdots \\ \left|x_i-x_1^*\right| & \cdots & \left|x_i-x_j^*\right| & \cdots & \left|x_i-x_m^*\right| \\ \vdots & & \vdots & & \vdots \\ \left|x_n-x_1^*\right| & \cdots & \left|x_n-x_j^*\right| & \cdots & \left|x_n-x_m^*\right| \end{bmatrix}, i=1,\ldots n,\ \ j=1,\ldots m \quad (1)$$

The purpose of this approach is to select the real peaks having its homologous in the set of theoretical peaks. For each x_i, the most similar value x_j^* is chosen if the difference between them is less than the tolerance θ, where an alarm could notice that the similitude has not been found. The minimum value of the components of each column $\mathbf{C}_j$ is given by a particular x_i. $\mathbf{X}_{\text{edges}}$ is a subset of $\mathbf{X}$ that contains the minimum values of each column **C**j, i.e.:

$$\mathbf{X}_{edges}=\left[\mathrm{x}_{edges1},\cdots,\mathrm{x}_{edges\,j},\cdots,\mathrm{x}_{edges\,m}\right]$$

$$\mathrm{x}_{edges,j}=x_r,\ x_r\in\mathbf{X}\ \ \forall\, r,j\ :\ c_{rj}=\min\left(\mathbf{C}_j\right)\leftrightarrow c_{rj}<\theta,\ j=1,2\ldots m \quad (2)$$

This method allows the determination of the absolute and relative error between the values obtained and expected for each event. The differences between the experimental and theoretical values are shown in Figure 10.

The peaks that do not have their counterpart with the theoretical peaks are possible echoes that come from a defect ($\mathbf{X}_{cracks}$).

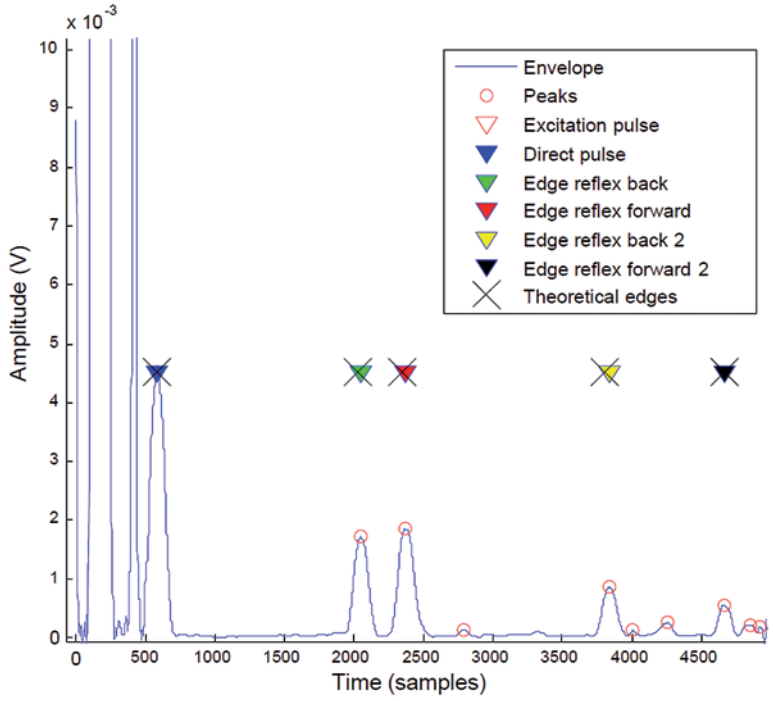

Fig. 10. Boundaries location using an algorithm which compares theoretical (cross) and experimental (triangle) values of ToF

$$\mathbf{X}_{cracks}\subseteq\mathbf{X}:\mathbf{X}_{cracks}\notin\mathbf{X}\cap\mathbf{X}_{edges} \quad (3)$$

$$\mathbf{X}_{cracks}=\left[\mathrm{x}_{cracks\,1},\cdots,\mathrm{x}_{cracks\,k},\cdots,\mathrm{x}_{cracks\,n-m}\right],\quad k=1,2,\ldots n-m$$

where the heights of $\mathbf{X}_{cracks}$ are:

$$\mathbf{Y}_{cracks}=\left[\mathrm{y}_{cracks\,1},\cdots,\mathrm{y}_{cracks\,k},\cdots,\mathrm{y}_{cracks\,n-m}\right],\quad k=1,2,\ldots n-m$$

The potential crack detection and location (see Figure 11) is based on the echoes that are coming from the same crack, where they could

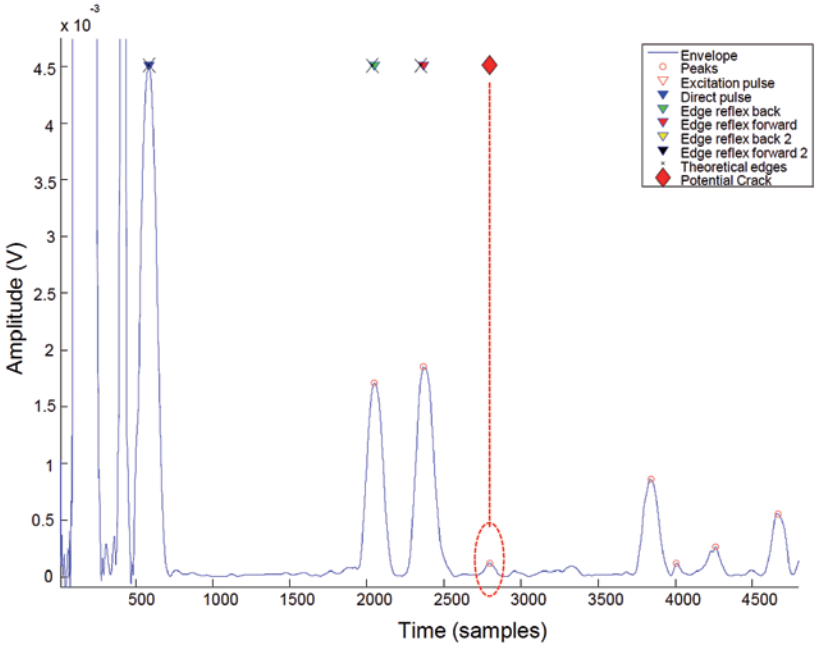

Fig. 11. Potential crack locations establishing relations between the two possible ways.

come from different paths due to the EMAT generate forward and reverse shear waves.

The algorithm considers that if the distance travelled is close, the defect is detected and therefore located. The scheme of this method is shown in Figure 12.

The pattern recognition approach is based on an automatic detection of cracks that compares the ToF employed by the same pulse to travel two different paths [18]. The two shortest paths for detecting a crack between the sensor and transmitter are the path "a" and path "b" shown in Figure 13. The distance travelled by an echo in the path "a", for example d_{echo_a}, is used to determine the distance drc_a between the crack and the receptor. Similarly, the distance travelled by an echo in the path "b" d_{echo_b} is used to determine the distance drc_b. The distances drc_a and drc_b should be close. The method performs a comparison between the distances obtained for each component of $\mathbf{X}_{cracks}$.

The paths are:

Path a:

$$d_{echo_{a,k}}=dtr+2dr+2drc_{a,k} \quad (4)$$

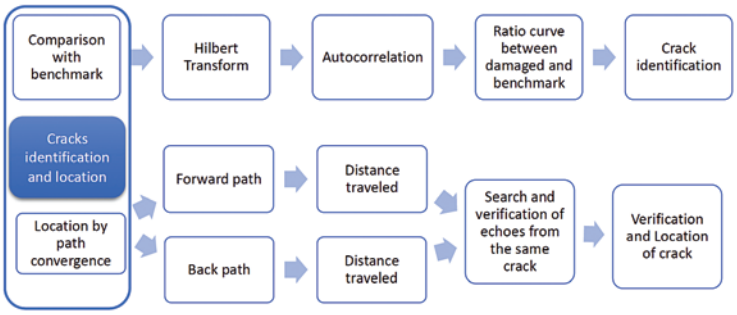

Fig. 12. Location of the crack by two methods: Comparison with "as commissioned" and; location by convergence of different paths

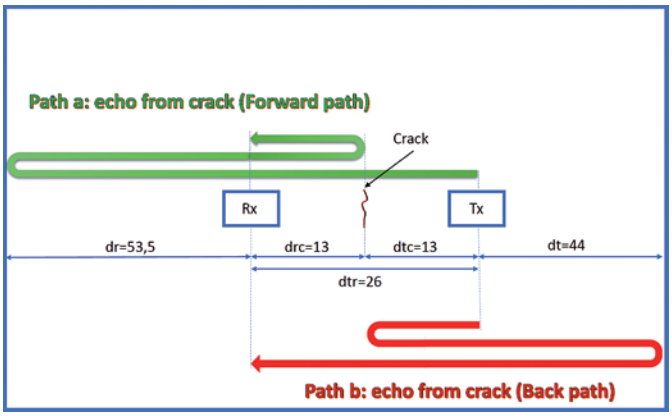

Fig. 13. Two shortest paths from Tx and Rx detecting the defect. The distance is given in centimetres

$$drc_{a,k} = \frac{d_{echo_{a,k}} - dtr - 2dr}{2} \tag{5}$$

$$\mathbf{D}\mathrm{rc}_{\mathrm{a}} = \left[drc_{a,1}, \cdots, drc_{a,k}, \cdots, drc_{a,m-n} \right], k = 1,2 \ldots n-m$$

Path b:

$$d_{echo_{b,k}} = 3dtc + 2dt + drc_{b,k} \tag{6}$$

$$dtc = dtr - drc_{b,k} \tag{7}$$

$$d_{echo_{b,k}} = 3(dtr - drc_{b,k}) + 2dt + drc \tag{8}$$

$$drc_{b,k} = \frac{3dtr + 2dt - d_{echo_{b,k}}}{2} \tag{9}$$

The distance $drc_{a,k}$ is compared with all the echoes that come from the path 2 ($drc_{b,k}$). Therefore, the pair of echoes that provide the most similar distances drc_1 and drc_2 have the greatest likelihood to come from the same defect.

$$\mathbf{D} = \begin{bmatrix} \left|d_{rc_{a,1}} - d_{rc_{b,1}}\right| & \cdots & \left|d_{rc_{a,1}} - d_{rc_{b,l}}\right| & \cdots & \left|d_{rc_{a,1}} - d_{rc_{b,n-m}}\right| \\ \vdots & & \vdots & & \vdots \\ \left|d_{rc_{a,k}} - d_{rc_{b,1}}\right| & \cdots & \left|d_{rc_{a,k}} - d_{rc_{b,l}}\right| & \cdots & \left|d_{rc_{a,k}} - d_{rc_{b,n-m}}\right| \\ \vdots & & \vdots & & \vdots \\ \left|d_{rc_{a,n-m}} - d_{rc_{b,1}}\right| & \cdots & \left|d_{rc_{a,n-m}} - d_{rc_{b,l}}\right| & \cdots & \left|d_{rc_{a,n-m}} - d_{rc_{b,n-m}}\right| \end{bmatrix}, \tag{10}$$

where $k = 1,2,\ldots,n-m, and\ l = 1,2,\ldots,n-m$. In some cases could appear superposition between two echoes that came from paths a and b, and therefore they would present in the signal as a single peak. The main diagonal provides the solution for these cases. The component $e_{crack\,k,l}$ is de minimum difference between both paths, given by:

$$e_{crack\,k,l} = d_{kl}: \quad d_{kl} = \min(\mathbf{D}) \leftrightarrow d_{kl} < \mathrm{t}, \quad \forall k,l. \tag{11}$$

The solution to the problem of location is $f_{crack,a}$, which is the distance of the crack from the sensor.

$$f_{crack,a} = drc_{a,k}, \ \forall\ k: \ d_{kl} = \min(\mathbf{D}) \leftrightarrow d_{kl} < \mathrm{t}, \quad \forall k,l. \tag{12}$$

The main diagonal is not taken into account for all other cases because it is assumed that there are no overlapping echoes. The difference between the $d_{rc_{a,k}}$ and $d_{rc_{b,l}}$ must be within the tolerance.

$$e_{crack} = d_{kl}: \quad d_{kl} = \min(\mathbf{D}): k \neq l \leftrightarrow \ \mathbf{D}_{kl} < \mathrm{t}, \forall k,l. \tag{13}$$

$$f_{crack,a} = drc_{a,k}, \ \forall\ k: \ d_{kl} = \min(\mathbf{D}): k \neq l \leftrightarrow d_{kl} < \mathrm{t}, \quad \forall k,l. \tag{14}$$

In some cases, there may be a need to consider the amplitude of each echo to perform the analysis. Theoretically an echo coming from a large transverse crack should have a greater amplitude than the echoes from smaller cracks, because more energy will be reflected.

The equation (15) weights the more similar distances with the amplitude of the two echoes of each path.

$$f^{w}_{crack,a} = drc_{a,k}, \ \forall\ k: \ d_{kl} = \min\left(\frac{\left|d_{rc_{a,k}} - d_{rc_{b,l}}\right|}{\mathrm{y}_{cracks\,k} + \mathrm{y}_{cracks\,l}} \right): k \neq l, \quad \forall k,l. \tag{15}$$

In most cases the amplitude of the echoes is several orders of magnitude smaller than the 'x' axis.

The equation (16) is a heuristic expression which gives more weight to the amplitude and corrects this problem.

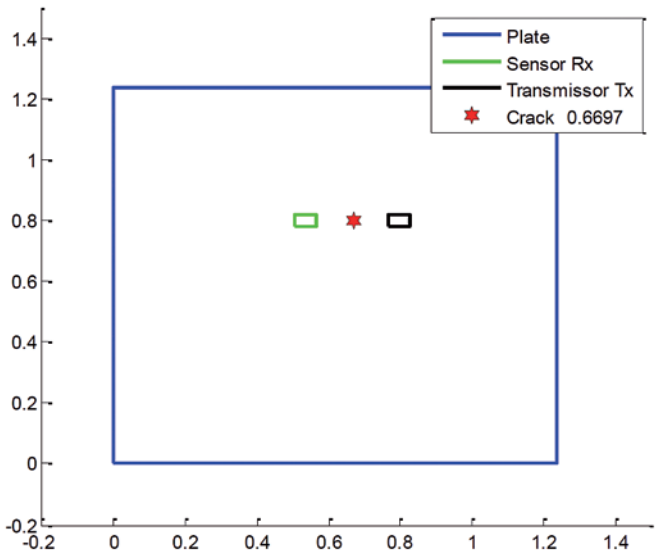

Fig. 14. Crack location relative to the left edge (meters)

$$f^{w}_{crack,a} = drc_{a,k},\ \forall\ k:\ \ d_{kl} = \min\left(\frac{\sqrt[g]{\left|d_{rc_{a,k}} - d_{rc_{b,l}}\right|}}{\left(y_{cracks\,k} + y_{cracks\,l}\right)^{g}}\right) \quad (16)$$

$$: k \neq l,\ \ \forall k,l,g$$

Finally, when the location is determined the crack is shown in a schematic with the actual dimensions of the plate and the position of the sensors (Figure 14).

5. Conclusions

This paper presents a new SHM approach using EMATs and advanced signal processing to automatically identify, locate and determine the severity of a defect in a plate. The technique presented could be used to detect defects in pipes operating under relatively high temperature. The approach employed is based on pre-filtering and denoising using Wavelet methodologies and the Hilbert Transform to detect relevant peaks. The Time of Flight (ToF) of the echoes is calculated theoretically and then compared with the experimental times to determine which echoes come from the plate borders. Any other echo represents a potential crack. Echoes from the same defect travelling on different paths are compared and the defect is located by taking consideration of the amplitude.

Acknowledgements

This work has been supported by the EU project INTERSOLAR (Ref.: FP7-SME-2013-605028) and the MINECO projects Ref.: RTC-2016-5694-3 and DPI2015-67264-P. The authors would like to thank Sonemat UK for their contribution to the manufacture of the EMAT transducers.

References

1. Aktas M, Turkmenoglu V. Wavelet-based switching faults detection in direct torque control induction motor drives. IET Science, Measurement & Technology 2010; 4(6): 303-310, https://doi.org/10.1049/iet-smt.2009.0121.
2. Canal M R. Comparison of wavelet and short time Fourier transform methods in the analysis of EMG signals. Journal of Medical Systems 2010; 34(1): 91-94, https://doi.org/10.1007/s10916-008-9219-8.
3. Chen Y. Acoustical transmission line model for ultrasonic transducers for wide-bandwidth application. Acta Mechanica Solida Sinica 2010; 23(2): 124-134, https://doi.org/10.1016/S0894-9166(10)60014-6.
4. Dai D, He Q. Structure damage localization with ultrasonic guided waves based on a time–frequency method. Signal Processing 2014; 96: 21-28, https://doi.org/10.1016/j.sigpro.2013.05.025.
5. Ruiz R, Garcia F P, Dimlaye V. Maintenance management of wind turbines structures via MFCs and wavelet transforms. Renewable and Sustainable Energy Reviews 2015; 48: 472-482, https://doi.org/10.1016/j.rser.2015.04.007.
6. Ruiz R, Garcia, F P, Dimlaye V, Ruiz D. Pattern recognition by wavelet transforms using macro fibre composites transducers. Mechanical Systems and Signal Processing 2014; 48(1): 339-350.
7. Dong Y, Shi H, Luo J, Fan G, Zhang C. Application of wavelet transform in MCG-signal denoising. Modern Applied Science 2010; 4(6): 20, https://doi.org/10.5539/mas.v4n6p20.
8. Eristi H. Fault diagnosis system for series compensated transmission line based on wavelet transform and adaptive neuro-fuzzy inference system. Measurement 2013; 46(1): 393-401, https://doi.org/10.1016/j.measurement.2012.07.014.
9. García F P, García I. Principal component analysis applied to filtered signals for maintenance management. Quality and Reliability Engineering International 2010; 26(6): 523-527, https://doi.org/10.1002/qre.1067.
10. García F P, Chacón J M, Tobias A M. B-Spline approach for failure detection and diagnosis on railway point mechanisms case study. Quality Engineering 2015; 27(2): 177-185, https://doi.org/10.1080/08982112.2014.933980.
11. García F P, Pedregal D J, Roberts C. Time series methods applied to failure prediction and detection. Reliability Engineering & System Safety 2010; 95(6): 698-703, https://doi.org/10.1016/j.ress.2009.10.009.
12. Genovese L, Neelov A, Goedecker S, Deutsch T, Ghasemi S A, Willand A. Schneider R. Daubechies wavelets as a basis set for density functional pseudopotential calculations. The Journal of chemical physics 2008; 129(1), https://doi.org/10.1063/1.2949547.
13. Jia M T, Wang Y C. Application of wavelet transformation in signal processing for vibrating platform. Journal-Shenyang Institute of Technology 2003; 22(3): 53-55.
14. Light-Marquez A, Sobin A, Park G, Farinholt K. Structural damage identification in wind turbine blades using piezoelectric active sensing. Structural Dynamics and Renewable Energy 2011; 1: 55-65, https://doi.org/10.1007/978-1-4419-9716-6_6.
15. Ljung L. System Identification Toolbox for Use with {MATLAB} 2007.
16. Marquez F P. An approach to remote condition monitoring systems management. Railway Condition Monitoring. The Institution of Engineering and Technology International Conference 2006: 156-160, https://doi.org/10.1049/ic:20060061.
17. Márquez F P. A New Method for Maintenance Management Employing Principal Component Analysis. Structural Durability & Health Monitoring 2010; 6(2): 89-99.
18. Márquez F P, Muñoz J M. A pattern recognition and data analysis method for maintenance management. International Journal of Systems Science 2012; 43(6): 1014-1028, https://doi.org/10.1080/00207720903045809.
19. Márquez F P, Pardo I, Nieto M. Competitiveness based on logistic management: a real case study. Annals of Operations Research 2013: 1-13.
20. Márquez F P G, Pedregal D J, Roberts C. New methods for the condition monitoring of level crossings. International Journal of Systems Science 2015; 46(5): 878-884, https://doi.org/10.1080/00207721.2013.801090.
21. Márquez F P, Pérez, J M, Marugán A P, Papaelias M. Identification of critical components of wind turbines using FTA over the time. Renewable Energy 2016; 87(2): 869–883, https://doi.org/10.1016/j.renene.2015.09.038.
22. Márquez F P, Tobias A M, Pérez J M, Papaelias M. Condition monitoring of wind turbines: Techniques and methods. Renewable Energy 2012; 46: 169-178, https://doi.org/10.1016/j.renene.2012.03.003.
23. Marugán A P, Márquez F P. A novel approach to diagnostic and prognostic evaluations applied to railways: A real case study.

Proceedings of the Institution of Mechanical Engineers, Part F: Journal of Rail and Rapid Transit 2016; 230(5): 1440-1456, https://doi.org/10.1177/0954409715596183.
24. Morsi W G, El-Hawary M E. Novel power quality indices based on wavelet packet transform for non-stationary sinusoidal and non-sinusoidal disturbances. Electric Power Systems Research 2010; 80(7): 753-759, https://doi.org/10.1016/j.epsr.2009.11.005.
25. Muñoz J, Márquez F P, Papaelias M. Railroad inspection based on ACFM employing a non-uniform B-spline approach. Mechanical Systems and Signal Processing 2013; 40(2): 605-617, https://doi.org/10.1016/j.ymssp.2013.05.004.
26. Nieto N, Marcela D. The use of the discrete Wavelet transform in the reconstruction of sinusoidal signals. Scientia et Technica 2008; 38: 381-386.
27. Papaelias M, Cheng L, Kogia M, Mohimi A, Kappatos V, Selcuk C, García F P, Gan T H. Inspection and Structural Health Monitoring techniques for Concentrated Solar Power plants. Renewable Energy2016; 85: 1178-1191, https://doi.org/10.1016/j.renene.2015.07.090.
28. Pedregal D J, García F P, Roberts C. An algorithmic approach for maintenance management based on advanced state space systems and harmonic regressions. Annals of Operations Research 2009; 166(1): 109-124, https://doi.org/10.1007/s10479-008-0403-5.
29. Peng Z K, Chu F L. Application of the wavelet transform in machine condition monitoring and fault diagnostics: a review with bibliography. Mechanical Systems and Signal Processing 2004; 18(2): 199-221, https://doi.org/10.1016/S0888-3270(03)00075-X.
30. Pérez, J. M. P., Márquez, F. P. G., & Hernández, D. R. (2016). Economic viability analysis for icing blades detection in wind turbines. Journal of Cleaner Production, 135, 1150-1160, https://doi.org/10.1016/j.jclepro.2016.07.026.
31. Pliego,A, García F P, Lorente J. Decision making process via binary decision diagram. International Journal of Management Science and Engineering Management 2015; 10(1): 3-8, https://doi.org/10.1080/17509653.2014.946977.
32. Su Z, Ye L. Identification of damage using Lamb waves: from fundamentals to applications Springer Science & Business Media 2009; 48.
33. Wang X, Peter W T, Mechefske C K, Hua M. Experimental investigation of reflection in guided wave-based inspection for the characterization of pipeline defects. NDT & E International 2010; 43(4): 365-374, https://doi.org/10.1016/j.ndteint.2010.01.002.
34. Wu J D, Liu C H. Investigation of engine fault diagnosis using discrete wavelet transform and neural network. Expert Systems with Applications 2008; 35(3): 1200-1213, https://doi.org/10.1016/j.eswa.2007.08.021.

Carlos Quiterio GÓMEZ Muñoz
Ingenium Research Group
European University of Madrid
Tajo street, C Building, C4 office, 28670, Villaviciosa de Odon
Madrid, Spain

Fausto Pedro GARCÍA Marquez
Alfredo ARCOS Jimenez
Ingenium Research Group
Castilla-La Mancha University
Politecnic Building, Camilo José Cela Street, 13071
Ciudad Real, Spain

Liang CHENG
Maria KOGIA
Abbas MOHIMI
Brunel Innovation Centre
TWI, Granta park, Granta Park
Cambridge, CB21 6AL
United Kingdom

Mayorkinos PAPAELIAS
School of Metallurgy and Materials
University of Birmingham
Edgbaston
Birmingham, B15 2TT
United Kingdom

E-mails: carlosquiterio.gomez@universidadeuropea.es, faustopedro.garcia@uclm.es, alfredo.arcos@alu.uclm.es, liang.cheng@brunel.ac.uk, maria.kogia@brunel.ac.uk, abbas.mohimi@brunel.ac.uk, m.papaelias@bham.ac.uk